Tellus (1989), *41B*, 272–285

A stochastic Lagrangian atmospheric transport model to determine global CO_2 sources and sinks—a preliminary discussion

By J. A. TAYLOR*, *Cooperative Institute for Research in Environmental Sciences, Campus Box 449, University of Colorado, Boulder, Colorado 80309 USA*

(Manuscript received 8 September 1987; in final form 16 January 1988)

ABSTRACT

A stochastic Lagrangian model describing the global tropospheric distribution of CO_2 is developed. Available source and sink terms are incorporated in the model. Advection terms are derived from the European Centre for Medium Range Weather Forecasting (ECMWF) analysed grids. Statistics for the variation in the advective terms are derived and incorporated in the model from the ECMWF data base. Model output is compared with CO_2 observations obtained from the National Oceanic and Atmospheric Administration (NOAA) Geophysical Monitoring for Climatic Change (GMCC) program. Model estimates of the yearly averaged latitudinal gradient of CO_2 concentration match the observed CO_2 concentrations except over the southern oceans. A biospheric growing season net flux (GSNF) of 6.5 Gt C was found, from model simulations, to explain the observed seasonal cycle in CO_2 concentrations. This value of the GSNF lies within the bounds of previous estimates. The intensity of the biospheric fluxes above 60° N, oceanic fluxes below 45° S and model vertical transport warrant further investigation.

1. Introduction

The determination of the fluxes associated with the sources and sinks of CO_2 remains an important problem in the study of the global carbon cycle. The difficulties associated with obtaining precise quantitative estimates of the biospheric and oceanic exchanges with the atmosphere by direct measurement or from theoretical considerations has led a number of researchers (Bolin and Keeling, 1963; Machta, 1972; Pearman and Hyson, 1980, 1986; Pearman et al., 1983; Heimann and Keeling, 1986; Fung et al., 1983, 1987) to attempt to infer from modelling studies, employing the best available transport data, a set of fluxes consistent with the observations of CO_2 in the atmosphere.

This approach has become increasingly sophisticated, in keeping with the constant improvement in the available atmospheric transport data (Lorenc, 1981), the expanding size of the data set of atmospheric CO_2 observations, and the availability of global distributions of the relative strength of the emissions of CO_2 from fossil fuel (Marland et al., 1985), biospheric CO_2 fluxes (Fung et al., 1987) and oceanic CO_2 fluxes (Takahashi et al., 1986). Current modelling approaches range from 1-dimensional models, being vertically and longitudinally averaged (Keeling and Heimann, 1986), 2-dimensional models which incorporate vertical as well as latitudinal variation (Pearman and Hyson, 1986) and 3-dimensional models (Fung et al., 1983, 1987; Walton et al., 1988) employing wind fields derived from a general circulation model (GCM).

The influence of regional and seasonal vari-

* Also Visiting Scientist at the National Center for Atmospheric Research, P.O. Box 3000, Boulder, CO 80307, USA. The National Center for Atmospheric Research is sponsored by the National Science Foundation.

tions in the global wind field on atmospheric concentrations can lead to significant differences between 2-dimensional model predictions and corresponding observations (Heimann and Keeling, 1986). Such differences may only be resolved by 3-dimensional models. Fung et al. (1987) consider that a 2-dimensional model cannot properly account for the longitudinal variations in CO_2 concentration and as a consequence must underestimate the biospheric fluxes required to obtain the observed CO_2 concentrations. Heimann and Keeling (1986) have suggested that such problems will be resolved by the use of multi-dimensional models of the general circulation based on a fine grid scale. Prather et al. (1987) noted the importance of developing 3-dimensional models to improve our understanding of atmospheric chemistry. Such models have been applied to the study of atmospheric chemistry for nearly 10 years (Mahlman and Moxim, 1978). A 3-dimensional Lagrangian model has recently been developed to treat the global-scale transport, transformation, and removal of trace species in the atmosphere (Walton et al., 1988).

In this paper, a 3-dimensional stochastic Lagrangian model is developed to describe the global atmospheric transport and concentration of CO_2. The model uses available estimates of the global distribution of anthropogenic CO_2 emissions, and biospheric and oceanic exchanges of CO_2. Various estimates of the magnitude of the biospheric and oceanic exchanges, based on values obtained in previous studies, are incorporated in the model. Model results are compared with NOAA/GMCC observations of atmospheric CO_2 concentrations.

The application of the Lagrangian modelling approach to the study of tracer concentrations on the global scale requires that a sufficiently large number of air parcels be available at each grid point to allow proper identification of air masses and to ensure that the fluxes associated with the sources and sinks of CO_2 are correctly represented. Accordingly, the model described here computes trajectories for some 100,000 air parcels.

The determination of trajectories of real air parcels becomes more uncertain with time. The trajectories computed by the model developed in this paper are intended to represent the mean circulation and variation about that mean. An individual trajectory is considered to represent one possible realization of an air parcel trajectory rather than a purely deterministic air parcel trajectory.

CO_2 was chosen as one of the tracer gases with which to study the model transport. CO_2 provides a sensitive test of model transport performance due to the complex interaction of the sources and sinks of CO_2 and the substantial seasonal and latitudinal variation in CO_2. In particular, the yearly averaged latitudinal gradient in the northern hemisphere is primarily determined by the well defined fossil fuel sources of CO_2. In addition, a comprehensive global set of CO_2 measurements are available with which to study model performance (Conway et al., 1988). Unfortunately uncertainties in the specification of the sources and sinks of CO_2 make the definitive validation of tracer transport difficult.

Other trace gases such as the chlorofluorocarbons (CFC's) have better defined source functions. However, CFC source functions are not free of uncertainty, particularly with regard to sources in the USSR. In addition, observations of CFC concentrations are relatively sparse when compared with available CO_2 measurements, and CFC concentrations exhibit very little seasonal variation. Accordingly, to more fully validate model transport, further work employing a range of trace gases, including CO_2, Radon, F-11, F-12 and methane, is currently being undertaken.

2. Modelling approach

The model developed in this study is based upon the Lagrangian tracer modelling approach. This modelling approach was adopted due to the following perceived advantages:

(1) the relative simplicity compared with the 3-dimensional eddy diffusion approach;

(2) the elimination of unwanted numerical diffusion associated with Eulerian approaches;

(3) multiple trace species can be advected simultaneously;

(4) the ability to easily track the trajectories of releases of chemical species within the model; and

(5) estimates of the variation in concentration associated with the wind field may be computed and compared with observations.

The availability of good estimates of observed global wind fields at a fine resolution (2.5 by 2.5 degrees) at a number of pressure levels was preferred to using GCM wind fields. The model takes advantage of modern computer architectures, particularly array processing. For example, model simulations of one year in duration with 100,000 air parcels on the CRAY X-MP/48 at the National Center for Atmospheric Research require only ~ 140 s of central processing time for completion.

While the Lagrangian modelling approach is considered to have the above advantages the approach is not without problems. A large number of air parcels are required to represent model transport on a model grid of fine resolution and to ensure that the fluxes of trace gases between the atmosphere and the sources and sinks are properly represented within the model. Also, as noted in the introduction, the determination of trajectories of real air parcels becomes more uncertain with time. The trajectories computed by the model represent the mean circulation and variation about that mean. An individual trajectory is then one possible realization of an air parcel trajectory rather than a purely deterministic air parcel trajectory.

The model must also satisfactorily represent transport in the polar regions and ensure that a Courant number less than one (Press et al., 1986) is realized for all grid cells. The problems associated with modelling the polar regions arise from the paucity of actual observations of the wind field and the close spacing of the model grid at the poles compared with the grid spacing at the equator. This may lead to a poor representation of the transport of CO_2 in these regions. The problem associated with the Courant number is that unless a value less than unity is maintained an air parcel may move over several grid cells in one time step thus producing an artificial advection. However, in the case of the Lagrangian approach, a Courant number greater than one will not lead to severe numerical instabilities, as can occur with a Eulerian model (Press et al., 1986).

The modelling approach adopted here uses a stochastic Lagrangian advection scheme to move air parcels representing a known mass of CO_2 in air according to a wind field on a 2.5 by 2.5 degree grid with seven vertical levels at 1000, 850, 700, 500, 300, 200 and 100 hPa which include a mean and time varying component. The flux of CO_2 into the atmosphere is computed based on estimates of fossil fuel emissions and exchange between the oceans and the biosphere. The flux of CO_2 is added or removed from air parcels present within the corresponding lowest level grid square of the model. Where an air parcel is not present in the lowest level grid square of the model during a time step, the flux of CO_2 not added in that time step is included in the next air parcel to arrive at the grid square. The residual flux was found to remain, at each time step, less than 1% of the total flux.

Accordingly, the location L, of particle p, in a grid cell located at latitude i, longitude j, level l and at time t is evaluated as

$$L^p_{ijlt} = L^p_{ijlt-1} + D^p_{ijlt} \tag{1}$$

where D^p_{ijlt} is the displacement of the particle occurring over 1 time step and is calculated for each wind speed component u, v and w independently according to

$$D^p_{ijlt} = \Delta t(\bar{m}_{ijl} + \bar{s}_{ijl} N(0,1)) \tag{2}$$

where Δt is the time step in seconds, $\bar{m}_{ijl}$ is the appropriate bi-monthly time period mean wind velocity (m s^{-1}) and $\bar{s}_{ijl}$ the standard deviation of wind velocity (m s^{-1}) over a bi-monthly time period derived at each grid point, and $N(0,1)$ represents a sample from the standard normal distribution.

The flux of CO_2 is evaluated for each grid cell F_{ijt} as

$$F_{ijt} = F^{\text{Anth.}}_{ijt} + F^{\text{Oceanic}}_{ijt} + F^{\text{Biospheric}}_{ijt}. \tag{3}$$

Seasonal cycles for the anthropogenic and biospheric fluxes were incorporated into the model. However, no seasonal cycle data were available with regard to oceanic CO_2 fluxes.

Mixing ratios were derived by translating the Lagrangian parcel coordinates to Eulerian grid coordinates. The Eulerian grid was based on the wind field grid. The divisions in the vertical were centred about the wind field pressure levels with the boundaries lying at the mid-point between the wind field pressure levels. The CO_2 concentration within each air parcel was then computed. The concentration on the Eulerian grid was calculated as the average of the air parcel concentrations within each grid.

For the Lagrangian method to be effective some form of diffusive mixing must be included in the model formulation (Walton et al., 1988). Without diffusive mixing the distribution of air parcel tracer concentrations would continue to broaden requiring increasing spatial and temporal averaging to obtain accurate estimates of tracer concentration. Diffusive mixing can be considered equivalent to allowing air parcels to interact by exchanging tracer mass or to allowing the boundaries of the air parcels to be slowly redefined (Walton et al., 1988).

Diffusive mixing is incorporated into the model by allowing tracer mass to be exchanged between air parcels. The exchange of tracer mass has been implemented by assigning the mass of tracer equivalent to the average concentration computed on the Eulerian grid to each air parcel within the corresponding grid cell. Calibration of such an approach to diffusive mixing, other than to the spatial distribution of tracer concentration, may be possible by comparing observed and predicted autocovariances of tracer concentration.

If should also be noted that, as the model employs the mass of tracer as the basic unit from which other quantities such as concentration are derived, the model conserves tracer mass. During model runs the mass of tracer within the model is computed at each time step. At the end of each time step and at the end of each model year the total mass of tracer exactly equals the starting mass plus the mass added attributed to sources of tracer minus the mass lost to the tracer sinks.

3. Wind field

Wind field data were obtained from the ECMWF in the form of a five year record of 0 h and 12 h observational analysis fields reported on a 2.5 by 2.5 degree grid. These data and the analysis procedures used to generate the data are described in detail by Lorenc (1981).

Rather than use the ECMWF data directly within the model, the data were reduced to a set of coefficients. In this way the computer model did not spend the majority of its execution time reading the wind field data. Based on theoretical grounds the components of the wind field should be normally distributed (Justus, 1978). In order to circumvent the problems associateed with non-stationarity in the wind fields due to seasonality, the year was divided into six bi-monthly intervals for which the parameters of the normal distributional model were estimated. It was considered that at least problems of severe non-stationarity could thus be avoided. An approximately sixty-fold reduction in wind field parameters required by the model could be achieved through this data reduction scheme.

In order to verify the validity of the hypothesis of normality a 2-month period of ECMWF data, beginning January 1980, was examined in detail. The test chosen to perform the analysis was the Kolmogorov–Smirnov test modified to take into account the estimation of the parameters (Lilliefors, 1967). Data sets consisting of a 60 day time series for each of the 3 wind components at each latitude, longitude and level were constructed and tested. The results, presented as the number of data sets accepted as normally distributed at the 95% confidence level for each wind component at each level, are reported as Table 1. In general, the results show that the hypothesis of normality is a reasonable assumption for the horizontal wind components.

However, the results for the vertical component show an apparent trend of increasing non-normality with height. Examination of the parameters of the distribution and the actual values reported by ECMWF for the vertical velocity component revealed that the data were reported to too few significant figures. This has

Table 1. *Number of data sets where the hypothesis of normality is accepted at the 95% confidence level**

At each pressure level 10,512 data sets consisting of 60 days of observations were derived beginning 1 January 1980 from the ECMWF 12 UT data base.

Wind speed component	Level (hPa)						
	1000	850	700	500	300	200	100
u	9028	9063	9192	9254	9190	9155	9087
v	9391	9465	9587	9489	9130	9306	9128
w	1433	6661	6625	6142	5375	2960	196

* The expected number of data sets which would be accepted at the 95% confidence interval if the data were normally distributed would be 9986.

produced a severe step function in the ordered data. The Kolmogorov–Smirnov test rejected the hypothesis of normality as the test is based on the assumption that the observations are drawn from a continuous distribution.

The correlation between the individual wind speed components of the ECMWF data were also examined. Accordingly, the cross correlation coefficient was computed for each of the 60 day time series at each latitude, longitude and level for u versus v, u versus w, and v versus w wind velocity components, where u refers to the east–west component, v the north–south component, and w the vertical velocity.

The number of data sets accepted as not cross correlated at the 95% and 99% confidence levels are reported in Table 2. For the u versus v, and u versus w wind velocity components only $\sim 15\%$ of all the data sets exhibit statistically significant cross correlation. For the v versus w components a high proportion of data sets appear to be significantly autocorrelated, particularly at the 500 hPa level. This result may again be due to the limited number of significant figures supplied by ECMWF for the reported values of the w component of wind velocity. However, the u versus w components showed no significant increase in the number of data sets rejected. Thus it would appear that the significant correlation of wind velocity may have arisen due to a slowly time varying v component correlating with a numerically rounded w component or as an artefact of the analysis procedure. A physical explanation for the above autocorrelation could be that the correlation has arisen as a consequence of the Hadley, Ferrel and polar circulations.

Unfortunately, without increasing the number of significant figures with which the w component is reported, selecting between the above explanations is difficult. However, given the high likelihood that the truncated w component data would contribute significantly to producing high cross correlation this explanation appears more likely. In this case the observed cross correlation would not greatly affect the model. This problem is currently the subject of further investigation.

Table 2. *Number of data sets where the hypothesis of cross correlation at the stated confidence level is rejected**

At each pressure level 10,512 data sets consisting of 60 days of observations were derived beginning 1 January 1980 from the ECMWF 12 UT data base.

	Confidence level (%)					
	u versus v		u versus w		v versus w	
Level (hPa)	95	99	95	99	95	99
1000	7164	8390	7706	8814	6721	7285
850	7579	8760	7173	8187	4658	5651
700	7913	8983	7594	8657	3634	4391
500	7882	8972	7390	8461	2974	3612
300	7201	8630	7748	8840	3324	4053
200	7177	8569	7786	9027	6034	6960
100	7238	8529	7932	9016	3771	4593

* The expected number of data sets where the hypothesis of cross correlation is rejected at the 95% confidence level would be 9986 if the data sets consisted of independent samples drawn from the normal distribution. At the 99% confidence level 10,406 would be rejected as not correlated.

4. Fossil fuel emissions of CO_2

Estimates of the fossil fuel emissions of CO_2 were based upon those derived by Marland et al. (1985). They produced a global distribution of CO_2 emissions for 1980 on a 5 degree grid. These values have been converted to fractions of the total emissions of CO_2 by Inez Fung (personal communication, 1987). Assuming that the distribution of fossil fuel emissions remains unchanged, the total fossil fuel emissions of CO_2 need only be applied on a year to year basis. This assumption is likely to remain valid for western countries however, Rotty (1987a) has noted particularly rapid growth in CO_2 emissions during the past decade from the developing countries.

Rotty (1987a) provides estimates of total CO_2 from fossil fuels for the period 1950–1984. It should be noted that his results for 1984 are provisional. In this paper interest is in the period 1980–1984 for which extensive global CO_2 observations are available. Rotty (1987a) also provides data for CO_2 emissions from the production of cement. These values have been included in the model according to the fossil fuel distribution due to the lack of the necessary globally gridded data with respect to the distribution of emissions from cement production. Cement production is esti-

mated to contribute about 2.5% of the total global CO_2 emission (Rotty, 1987a).

An important aspect of any model attempting to explain the observed CO_2 concentrations is a proper description of the seasonal cycle of CO_2 emissions. This cycle in CO_2 concentration is particularly noticeable in the northern hemisphere whilst attenuated in the southern hemisphere. Rotty (1987b) has studied the seasonal cycle of fossil fuel emissions of CO_2 based on 87% of the total CO_2 emissions for the year 1982. Rotty (1987b) computed estimates of the percentage of the total fossil fuel emissions of CO_2 for each month of 1982. A maximum value of 9.56% was obtained in January 1982 reflecting the demand for heating during the northern hemisphere winter, while the minimum value of 7.56% occurred in August 1982. This seasonal cycle of fossil fuel emissions of CO_2 has been incorporated into the model developed in this paper. This seasonal cycle complements the biospheric seasonal cycle. As a consequence the two cycles act together to amplify the observed seasonal cycle of CO_2 concentration however, the effect of seasonality in fossil fuel emissions should be small when compared with the biospheric seasonal cycle.

5. Biospheric CO_2 exchange function

The precise specification of a biospheric exchange function has yet to be achieved. This is due in part to the lack of quantitative modelling of this exchange and the difficulties associated with interpreting CO_2 observations obtained adjacent to, or in the middle of, the oceans rather than in the centre of biospheric exchange on the continents.

Several estimates of the growing season net flux (GSNF), defined as the net flux of CO_2 to the biosphere, have been obtained in various studies. These estimates, which vary by a factor of 3, are listed as Table 3. The Fung et al. (1983, 1987) estimates are the largest. Only Fung et al. (1983, 1987) have employed a 3-dimensional model in deriving their estimates of GSNF. They have argued that 2-dimensional models must underestimate the GSNF required to obtain the observed values at remote locations as such models do not properly account for the longitudinal variation in GSNF. However, a 3-dimensional model will not necessarily provide an accurate estimate of GSNF unless the longitudinal transport is accurately represented. With the present data base of atmospheric CO_2 observations dominated by measurements at ocean sites, underestimation of the longitudinal transport will produce a higher estimate of GSNF while overestimation will produce a lower estimate of GSNF.

Table 3. *Estimates of the growing season net flux (GSNF) obtained from various studies*

GSNF (Gt C)	Study
4.1	Bolin and Keeling (1963)
4.21	Machta (1972)
6.06	Pearman and Hyson (1986)
6.35	Pearman and Hyson (1980)
9.3	Fung et al. (1987)
13.0	Fung et al. (1983)

Pearman and Hyson (1986) believe that the results of Fung et al. (1983) can be explained by the rapid vertical mixing incorporated in the Fung et al. (1983) 3-dimensional transport model. Pearman and Hyson (1986) consider that their model has realistically represented the vertical transport of CO_2. However, the data they employed was limited and may not be representative of the global behaviour of the atmosphere or, most importantly, of the source areas of CO_2.

Fung et al. (1987) derived estimates of the biospheric flux of CO_2 on a global 4.5 by 5 degree grid on a monthly basis. These estimates of biospheric fluxes have been interpolated to the 2.5 by 2.5 degree grid of the Lagrangian tracer transport model. The estimates of the biospheric fluxes of CO_2, as derived by Fung et al. (1987), assume that a zero net flux will be obtained between the biosphere and the atmosphere if the fluxes are averaged over one year. As the model developed in this study is 3-dimensional, the Fung et al. (1987) value for GSNF was initially employed. However, model results indicated that a value of 6.5 Gt C, spatially distributed relative to the Fung et al. (1987) estimates, would best reproduce CO_2 observations. This value lies within the bounds of previous estimates of the GSNF, as listed in Table 3.

6. Ocean CO_2 fluxes

The flux of CO_2 between the oceans and the atmosphere has been determined according to the following expressions (Smethie et al., 1985)

$$F = q \cdot Vp(CO_2) \cdot \alpha(CO_2) \cdot \Delta pCO_2 \quad (4)$$

where q is a chemical enhancement factor for the exchange of CO_2, $Vp(CO_2)$ is the piston velocity of CO_2, $\alpha(CO_2)$ is the solubility of CO_2 in sea water, and ΔpCO_2 is the difference in CO_2 partial pressures between sea water and air. Smethie et al. (1985) suggest a value of 1.0 for the chemical enhancement factor. Based on the data listed in Table 2 of Smethie et al. (1985) an average value for the piston velocity of 4.95 m day^{-1} was derived, while for the CO_2 solubility a mean value of 28.1 M m^{-3} atm^{-1} was obtained. The mean values of the piston velocity and CO_2 solubility, which is very temperature dependent, were obtained by Smethie et al. (1985) in the region 10°S to 30°N. Hence the piston velocities and the CO_2 solubilities may be underestimated for the southern and northern oceans. However, assuming that the flux into the oceans is greater than the flux leaving the oceans by an amount equivalent to 44% of the total anthropogenic emissions of CO_2 (Keeling and Heimann, 1986) the flux into the northern and southern oceans may be balanced against the flux generated in the equatorial regions for which estimates of the piston velocity and CO_2 solubility are available. Using these values, eq. (4) above reduces to

$$F = 1.39 \times 10^{-4} \Delta pCO_2 \text{ (moles m}^{-2} \text{ day}^{-1}) \quad (5)$$

where ΔpCO_2 is in units of μatm.

In order to compute the fluxes according to eq. (5) estimates of ΔpCO_2 must be obtained. Takahashi et al. (1986) have obtained estimates of the seasonal mean ΔpCO_2 for the various oceanic regions of the globe. These data, on a 10 by 10 degree grid, have been interpolated to the 2.5 by 2.5 degree grid of the model developed in this paper.

Using the data of Takahashi et al. (1986) and eq. (5) the regions of negative and positive net fluxes between the atmosphere and the oceans were computed. These fluxes were −2.378 Gt C and 1.822 Gt C with respect to the atmosphere. The net flux of CO_2 from the equatorial regions was approxiamtely 1.6 Gt C. This value is consistent with that obtained by Keeling and Heimann (1986). Pearman et al. (1983) have estimated that the equatorial oceans represented a source of about 2 Gt C. The estimate of the flux of 1.6 Gt C from the equatorial oceans has been adopted in this study. Based on the assumption of a global net flux from the atmosphere to the oceans of 44% of the total anthropogenic emissions of CO_2 (Keeling and Heimann, 1986), and the assumption that the net flux into the atmosphere in the equatorial regions is more reliably estimated, all negative fluxes were multiplied by a factor to yield a net flux from the atmosphere of 44% of the total anthropogenic emissions of CO_2.

Pearman and Hyson (1986) have noted that the oceanic fluxes of CO_2 in the southern hemisphere exhibit an annual seasonal cycle leading to an atmospheric cycle of amplitude of about 1 ppm. However, lacking any information on the spatial variation of this seasonal cycle, this cycle was not included in the model developed in this study.

7. Atmospheric CO_2 measurements

Conway et al. (1988) report CO_2 concentrations determined from flask samples collected at the 22 NOAA/GMCC monitoring sites for 1981–1984. Komhyr et al. (1985) detail the NOAA/GMCC monitoring program and report the results of the program from its commencement in 1968 until 1982. The locations of these monitoring sites are listed in Table 4 and presented in Fig. 1. The monitoring sites are in general located near the oceans in the atmospheric boundary layer and are remote from the major sources and sinks of CO_2.

Several important features of the spatial distribution of CO_2 concentration and its variation have been characterized by Conway et al. (1988). The features of particular interest in this study are the latitudinal gradient of the CO_2 concentration, the amplitude of the seasonal cycle of CO_2 concentration and its variation with latitude, and the net increase in CO_2 concentration.

The air samples obtained by Conway et al. (1988) were collected for the purpose of determining "background" CO_2 concentrations so that global trends in CO_2 concentration could be evaluated. Accordingly, Conway et al. (1988)

Table 4. *Location of National Oceanic and Atmospheric Administration (NOAA) Geophysical Monitoring for Climatic Change (GMCC) flask sampling sites**

Site code	Site	Latitude (degrees)	Longitude (degrees)	Elevation (metres)
AMS	Amsterdam Is., Indian Ocean	38 S	78 E	54
ASC	Ascension Is., S. Atlantic	8 S	14 W	54
AVI	St. Croix, Virgin Islands	18 N	65 W	3
AZR	Azores (Terceira Is.), North Atlantic	39 N	27 W	30
BRW	Point Barrow, Alaska	71 N	157 W	11
CBA	Cold Bay, Alaska	55 N	163 W	25
CGO	Cape Grim, Tasmania	41 S	145 E	94
CHR	Christmas Island	2 N	157 W	3
CMO	Cape Meares, Oregon	45 N	124 W	30
GMI	Guam, North Pacific	13 N	145 E	2
HBA	Halley Bay, Antarctica	75 S	27 W	3
KEY	Key Biscayne, Florida	26 N	80 W	3
KUM	Cape Kumukahi, Hawaii	20 N	155 W	3
MBC	Mould Bay, Canada	76 N	119 W	15
MLO	Mauna Loa, Hawaii	20 N	156 W	3397
NWR	Niwot Ridge, Colorado	40 N	106 W	3749
NZL	Kaitorete Spit, New Zealand	44 S	173 W	3
PSA	Palmer Station, Antarctica	65 S	64 W	33
SEY	Seychelles, Indian Ocean	5 S	55 E	3
SMO	American Somoa, South Pacific	14 S	171 W	30
SPO	Amundsen Scott, South Pole	90 S	—	2810
STM	Station "M", North Atlantic	66 N	2 E	6

* Adapted from Conway et al. (1988).

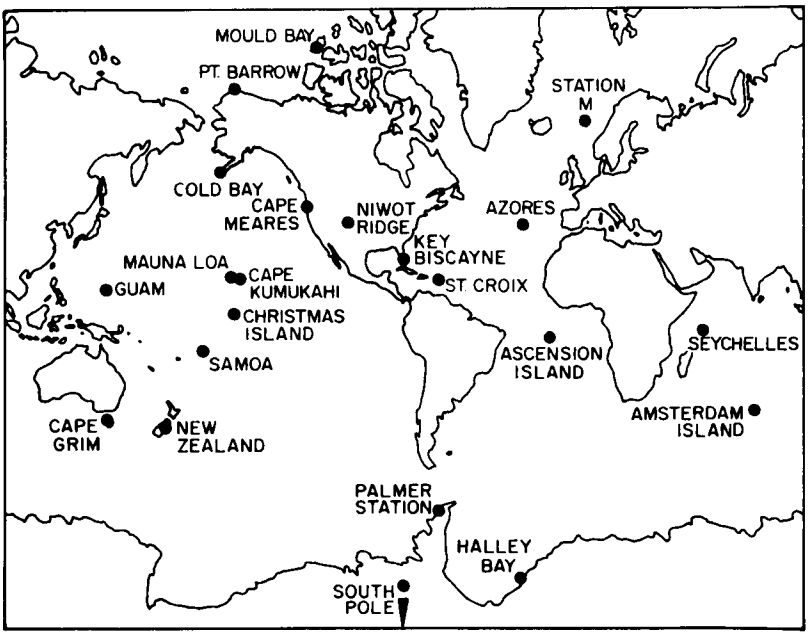

Fig. 1. Map of the NOAA/GMCC flask sampling sites (from Conway et al., 1988).

have collected air samples within specified wind sectors, at wind speeds greater than some minimum value and at a particular time of day at many sites. This makes the direct comparison of the Conway et al. (1988) data with model results problematic as the model predictions would have to take into account the conditions under which the CO_2 measurements were obtained. However, these CO_2 measurements do provide a useful guide to the variation of atmospheric CO_2 concentration.

8. Results and discussion

The model, with the fossil fuel emission of CO_2, oceanic and biospheric fluxes of CO_2 described earlier, was run for a time period of 24 months with a time step of 24 hours and 100,000 air parcels. The time step is a model parameter which can be adjusted to suit the application. Clearly, the shorter the model time step the more accurate the computed trajectories. The model time step of 24 hours was selected as the wind field is based on 24 hour average data and as monthly and annual mean concentrations of a long lived trace gas, CO_2, are the model results of interest.

The model was initialized in a standard manner (Pearman and Hyson, 1986; Fung et al., 1983). The monthly mean CO_2 concentration values for the month of January 1984 were used to prescribe a concentration field varying with latitude. The last 12 months of model results are presented in the following discussion. The first 12 months of model running time was required to ensure that the effects of model initialization were overcome to produce a realistic concentration distribution.

The results of the model run are compared with the observations of CO_2 concentration collected from NOAA/GMCC flask monitoring network (Conway et al., 1988). Fig. 2 presents the latitudinal variation of annual mean CO_2 concentration obtained from the model simulation and the NOAA/GMCC flask network sites for 1984. This annual mean latitudinal profile is determined by fossil fuel emissions and oceanic fluxes of CO_2. Fig. 2 demonstrates that the model developed in this study provides a good representation of the observed latitudinal gradient except over the

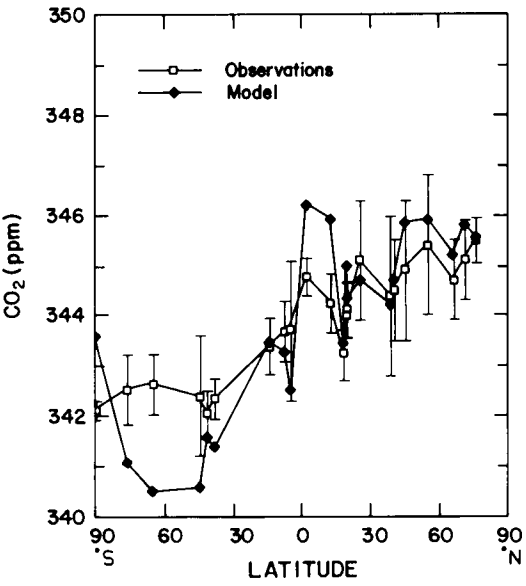

Fig. 2. Latitudinal variation of annual mean CO_2 concentration for the NOAA/GMCC flask sampling sites for 1984 and corresponding model predictions. Error bars correspond to $2\bar{\sigma}_s$ where $\bar{\sigma}_s$ is the mean of the monthly σ_s values reported in Table 3 of Conway et al. (1988).

southern oceans and equatorial regions. This deviation is significant below about 40°S. Takahashi et al. (1986) predict an intense sink region for CO_2 in the southern oceans. This intense sink of CO_2 may be overestimated leading to model predictions of CO_2 concentrations falling below those observed at the NOAA/GMCC sites. This result may imply a particularly poor model representation of vertical mixing in this region.

Figs. 3–6 show examples of the modelled cycles of atmospheric CO_2 concentration at locations corresponding to sixteen NOAA/GMCC flask network sites together with the observed annual cycles, recorded during 1984, at these sites (Conway et al., 1988). Model predictions have been adjusted by the difference between the observed and predicted January CO_2 concentrations. Again, it should be noted that the CO_2 concentrations recorded at the NOAA/GMCC flask network sites represent a selected sample of actual atmospheric CO_2 concentrations occurring at these sites. It is not expected then that model predictions and observations will agree exactly.

Fig. 3 presents the results obtained at the northern latitude sites, namely Mould Bay, Point Barrow, Ocean Station "M" and Cold Bay. At all four sites a departure of model predictions from the observed concentrations during the months of May and June has occurred. However, the amplitude of the seasonal cycle is reasonably well predicted. In general, this over-prediction in May and June is attenuated with decreasing latitude. It is considered that the high concentrations predicted by the model in the northern latitudes can be attributed to the biospheric source of CO_2 being too intense at these latitudes during May and June. Alternatively poor representation of vertical mixing or transport to and from mid-northern latitudes may produce the elevated CO_2 concentrations predicted by the model. Further work with trace gases for which vertical profiles are available, such as Radon, will be required to resolve this problem.

Fig. 4 presents the model results obtained at the mid-northern latitude sites at Cape Meares, Niwot Ridge, Cape Kumukahi and Key Biscayne. The predictions of concentration at Niwot Ridge have been derived as estimates of the 700 hPa concentration as Niwot Ridge is at an elevation of 3,749 metres. Overestimation of the intensity of the seasonal cycle by the model

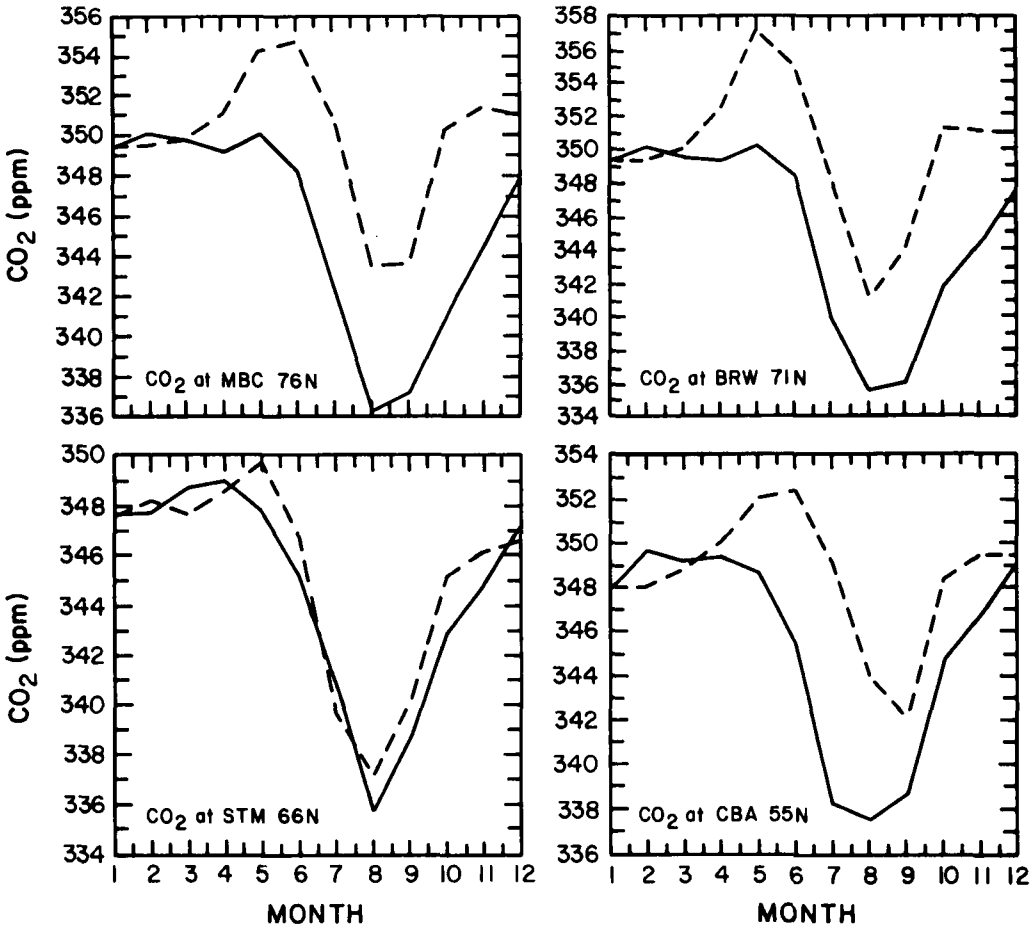

Fig. 3. Monthly mean CO_2 concentrations at four northern latitude NOAA/GMCC flask sampling sites (—) and corresponding model predictions (– –).

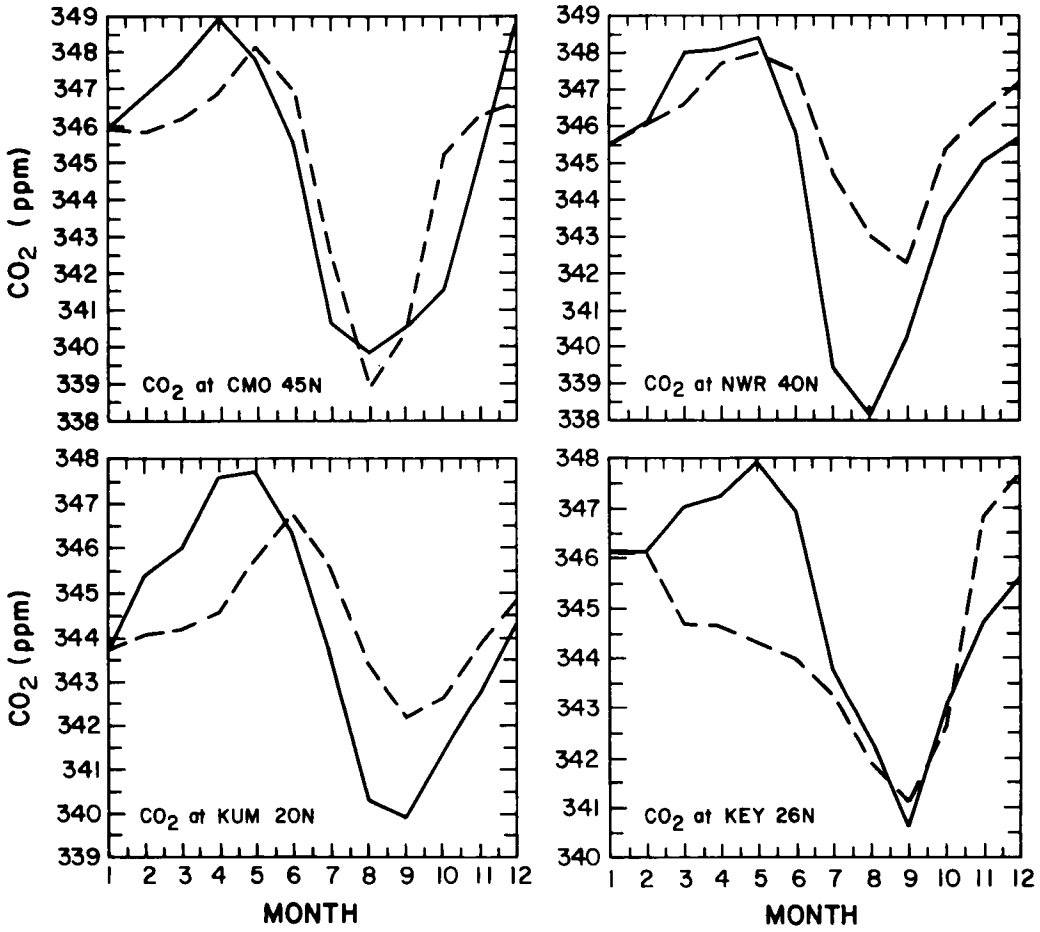

Fig. 4. Monthly mean CO_2 concentrations at four mid-northern latitude NOAA/GMCC flask sampling sites (—) and corresponding model predictions (– –).

would be anticipated if the surface concentration estimates were employed. Such a result is to be expected based on the study conducted by Tanaka et al. (1983) who found that the amplitude of the seasonal cycle decreases with increasing altitude. Pearman and Hyson (1986) note that some uncertainty surrounds whether the Niwot Ridge site should be considered as measuring the CO_2 concentration of lower or mid-troposphere air. A further problem confounding the interpretation of model results at Niwot Ridge is that the ECMWF analysis wind fields are reported at pressure levels which do not take into account the effects of topography. The results obtained here indicate that the predicted 700 hPa concentrations underestimate the amplitude of the seasonal cycle at Niwot Ridge. However, it is recognized that source and sink terms that were too large or underestimation of the vertical transport of CO_2 in this region could produce the same model results.

Fig. 5 presents the model predictions for the equatorial sites at St. Croix, Guam, Christmas Island and Ascension Island. The intense oceanic CO_2 source region incorporated in the model (1.6 Gt C) lies in the equatorial waters between 10°N and 10°S.

Finally, Fig. 6 presents the results for the southern latitude NOAA/GMCC sites at Amsterdam Is., Cape Grim, Kaitorete Spit and Halley

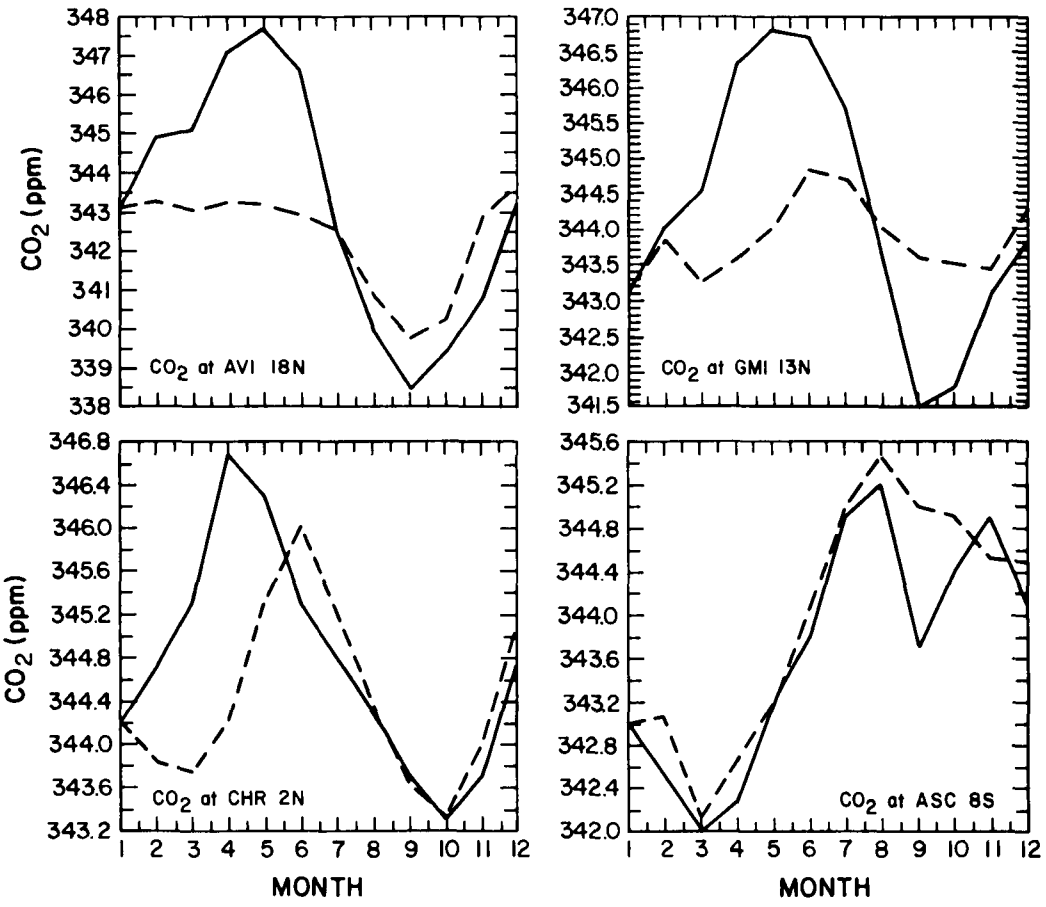

Fig. 5. Monthly mean CO_2 concentrations at four equatorial NOAA/GMCC flask sampling sites (—) and corresponding model predictions (- -).

Bay. The southern oceans are considered by Takahashi et al. (1986) as a major sink for CO_2 particularly below 40°S. The model has reproduced the ~1 ppm amplitude of the seasonal cycle observed at Cape Grim without including a seasonal cycle for the oceanic fluxes of CO_2 as suggested by Pearman and Hyson (1986). However, underestimation of model vertical mixing would contribute to producing this result.

9. Conclusions

A stochastic Lagrangian modelling approach has been developed and model estimates of the CO_2 concentration have been compared with those observed in the atmosphere at NOAA/GMCC monitoring locations. Estimates of the equatorial flux of CO_2 from the oceans to the atmosphere of 1.6 Gt C and the biospheric GSNF of 6.5 Gt C were found, from model simulations, to explain observed CO_2 concentrations. This estimate of the GSNF represents a minimum bound as a parameterization for subgrid scale vertical mixing has yet to be included within the model formulation. The intensity of the biospheric fluxes above 60°N and of oceanic fluxes below 45°S warrant further investigation.

This study, in keeping with earlier studies (e.g. Fung et al., 1987; Pearman and Hyson, 1986;

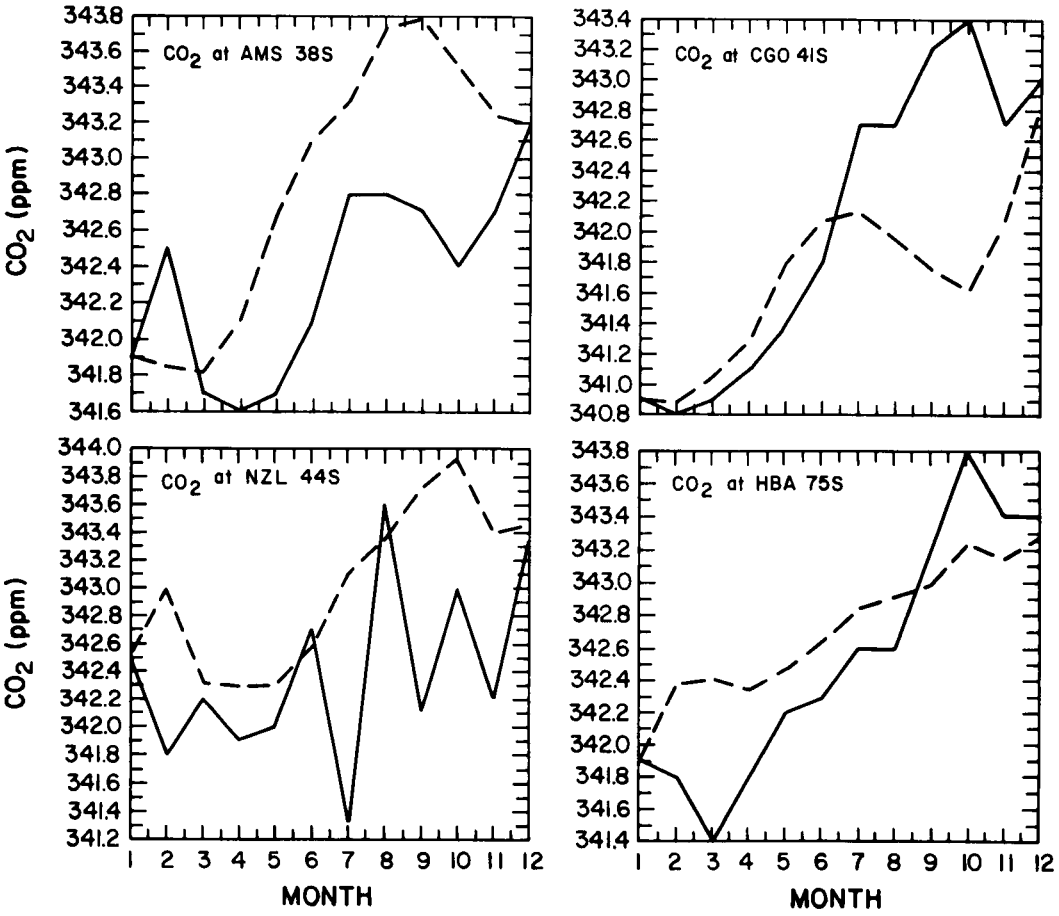

Fig. 6. Monthly mean CO_2 concentrations at four southern latitude NOAA/GMCC flask sampling sites (—) and corresponding model predictions (– –).

Keeling and Heimann, 1986) has found that the estimation of the above source terms are subject to uncertainties in the definition of the transport component of the atmospheric model. With the exception of the vertical velocity component of wind speed the estimates of advection adopted in this study are based on actual measurements which have been analysed to provide a global grid of wind speeds. However, the definition of vertical velocity remains very uncertain particularly with respect to sub-grid scale phenomena such as storms where rapid vertical mixing can occur. The problem of obtaining good estimates of vertical velocity is made more difficult by the absence of an extensive set of observations of the vertical concentration profile of CO_2 with which vertical velocity could be calibrated.

10. Acknowledgements

The author would like to thank Inez Fung who provided data on the distribution of fossil fuel and biosphere CO_2 fluxes, and Guy Brasseur, Richard Brost and Bob Chatfield for many useful discussions. The European Centre for Medium Range Weather Forecasting provided a substantial data set of global wind fields. The author would like to thank Cedo Brankovic of ECMWF for discussions concerning the ECMWF data set.

The author also greatly appreciated the many excellent comments of the referees. Finally this work would not have been possible without the support of the National Oceanic and Atmospheric Administration's Geophysical Monitoring for Climatic Change program.

REFERENCES

Bolin, B. and Keeling, C. D. 1963. Large-scale atmospheric mixing as deduced from the seasonal and meridional variations of carbon dioxide. *J. Geophys. Res. 68*, 3899–3920.

Conway, T. J., Tans, P., Waterman, L. S., Thoning, K. W., Masarie, K. A. and Gammon, R. H. 1988. Atmospheric carbon dioxide measurements in the global troposphere, 1981–1984. *Tellus 40B*, 81–115.

Fung, I., Prentice, K., Matthews, E., Lerner, J. and Russel, G. 1983. Three-dimensional tracer model study of atmospheric CO_2: Response to seasonal changes with the terrestrial biosphere. *J. Geophys. Res. 88*, 1281–1294.

Fung, I. Y., Tucker, C. J. and Prentice, K. C. 1987. Application of advanced very high resolution radiometer vegetation index to study atmosphere–biosphere exchange of CO_2. *J. Geophys. Res. 92*, 2999–3015.

Heimann, M. and Keeling, C. D. 1986. Meridional eddy diffusion model of the transport of atmospheric carbon dioxide 1. Seasonal carbon cycle over the tropical Pacific Ocean. *J. Geophys. Res. 91*, 7765–7781.

Justus, C. G. 1978. *Winds and wind system performance*. Philadelphia, PA: The Franklin Institute Press.

Keeling, C. D. and Heimann, M. 1986. Meridional eddy diffusion model of the transport of atmospheric carbon dioxide 2. Mean annual carbon cycle. *J. Geophys. Res. 91*, 7782–7796.

Komyhr, W. D., Gammon, R. H., Harris, T. B., Waterman, L. S., Conway, T. J., Taylor, W. R. and Thoning, K. W. 1985. Global atmospheric CO_2 distribution and variations from 1968–1982 NOAA/GMCC CO_2 flask sample data. *J. Geophys. Res. 90*, 5567–5596.

Lilliefors, H. W. 1967. On the Kolmogorov–Smirnov test for normality with mean and variance unknown. *J. of the Amer. Stat. Assoc. 62*, 399–402.

Lorenc, A. C. 1981. A global three-dimensional multivariate statistical interpolation scheme. *Mon. Wea. Rev. 109*, 701–721.

Machta, L. 1972. Mauna Loa and global trends in air quality. *Bull. Am. Met. Soc. 53*, 402–420.

Mahlman, J. D. and Moxim, W. J. 1978. Tracer simulation using a global general circulation model: Results from a mid-latitude instantaneous source experiment. *J. Atmos. Sci. 35*, 1340–1378.

Marland, G., Rotty, R. M. and Treat, N. L. 1985. CO_2 from fossil fuel burning: global distribution of emissions. *Tellus 37B*, 243–258.

Pearman, G. I. and Hyson, P. 1980. Activities of the global biosphere as reflected in atmospheric CO_2 records. *J. Geophys. Res. 85*, 4457–4467.

Pearman, G. I. and Hyson, P. 1986. Global transport and inter-reservoir exchange of carbon dioxide with particular reference to stable isotopic distributions. *J. Atmos. Chem. 4*, 81–124.

Pearman, G. I., Hyson, P. and Fraser, P. J. 1983. The global distribution of atmospheric carbon dioxide: 1. Aspects of observations and modeling. *J. Geophys. Res. 88*, 3581–3590.

Prather, M., McElroy, M., Wofsy, S., Russel, G. and Rind, D. 1987. Chemistry of the global troposphere: fluorocarbons as tracers of air motion. *J. Geophys. Res. 92*, 6579–6613.

Press, W. H., Flannery, B. P., Teukolsky, S. A. and Vetterling, W. T. 1986. *Numerical Recipes: The art of scientific computing*. Cambridge: University Press.

Rotty, R. M. 1987a. A look at 1983 CO_2 emissions from fossil fuels (with preliminary data for 1984). *Tellus 39B*, 203–208.

Rotty, R. M. 1987b. Estimates of seasonal variation in fossil fuel CO_2 emissions. *Tellus 39B*, 184–202.

Smethie, W. M. Jr., Takahashi, T., Chipman, D. W. and Ledwell, J. R. 1985. Gas exchange and CO_2 flux in the tropical Atlantic Ocean determined from 222Rn and pCO_2 measurements. *J. Geophys. Res. 90*, 7005–7022.

Takahashi, T., Goddard, J., Sutherland, S., Chipman, D. W. and Breeze, C. 1986. Seasonal and geographic variability of carbon dioxide sink/source in the oceanic areas: observations in the north and equatorial Pacific Ocean, 1984–1986 and global summary. Final Technical Report for Contract MRETTA 19X-89675C submitted to Carbon Dioxide Research Division Office of Energy Research, United States Department of Energy, Washington DC 20545 and Global Carbon Cycle Program Oak Ridge National Laboratory, Oak Ridge, TN 37839, USA.

Tanaka, M., Nakazawa, T. and Aoki, S. 1983. Concentration of atmospheric carbon dioxide over Japan. *J. Geophys. Res. 88*, 1339–1344.

Walton, J. J., MacCracken, M. C. and Ghan, S. J. 1988. A global-scale Lagrangian trace species model of transport, transformation, and removal processes. *J. Geophys. Res. 93*, 8339–8354.